THERMAL FATIGUE BEHAVIOR OF ASPHALT CONCRETE UNDER CONSTANT AMPLITUDE STRAIN LOADING

Ali Arabzadeh
Department of Civil Engineering
Middle East Technical University
Dumlupınar Blvd. 06800 Ankara, Turkey
Tel: +90 (312) 210-5482 Fax: +90 (312) 210-5401; Email: ali.arabzadeh@metu.edu.tr

Yalçın Karakaya
Department of Civil Engineering
Middle East Technical University
Dumlupınar Blvd. 06800 Ankara, Turkey
Tel: +90 (312) 210-7442 Fax: +90 (312) 210-5401; Email: kayalcin@metu.edu.tr

Murat Guler, Corresponding Author
Department of Civil Engineering
Middle East Technical University
Dumlupınar Blvd. 06800 Ankara, Turkey
Tel: +90 (312) 210-2464 Fax: +90 (312) 210-5401; Email: gmurat@metu.edu.tr

Word count: 4,864 words text + 14 tables/figures x 250 words (each) = 8364

Submission Date: November 17, 2014

ABSTRACT

Thermal fatigue is another form of thermally induced distress in flexible pavements, leading to serious degradations of structural performance and service quality of roadways. Thermal fatigue cracks occur in moderate climates with considerable temperature variations and are the result of generated cyclic thermal strains/stresses within the restrained pavement layers. In this study, an experimental setup is developed in order to measure the thermal fatigue resistance of asphalt concrete specimens under constant strain amplitude loading. The test specimens are aged in the laboratory for a long duration of time and include variations of aggregate source, gradation, asphalt binder and asphalt content. To simulate thermal fatigue behavior of asphalt concrete, uniaxial loading is mechanically applied to achieve constant amplitude sinusoidal strains at a frequency of 0.01Hz. The strain amplitudes are calculated based on the measured thermal coefficients of the test specimens and the temperature differential corresponding to highest frequency for the city of Ankara. The results of experiments used in the statistical analysis of variance include three response parameters as 35 % reduction of its initial stiffness, 50% reduction of its initial stiffness and the rate of reduction in the stiffness of the specimens. The results of statistical analyses indicate that the among the mixture design variables included in the testing program, the asphalt content, aggregate source and asphalt binder type have the strongest effect on the thermal fatigue resistance of asphalt concrete.

Keywords: Thermal Fatigue Resistance, Asphalt Concrete, Thermal Expansion Coefficient, Strain Loading

INTRODUCTION

Thermal cracking can cause considerable deteriorations in the structural and functional performance of asphalt concrete pavements. The thermal stress developed in asphalt concrete is attributed to the volume change characteristics of mixture which is defined by its thermal contraction/expansion behavior (*1*). The temperature differentials produce thermal strains and because of the restraint due to the friction between asphalt concrete layer and its underlying layer, thermal stresses are generated and eventually cause top to bottom cracking in the surface course. The cracks in the surface course, if not rehabilitated, can lead to severe structural problems and loss of service quality of roadways. Because of their significant impact on pavement performance, thermally induced cracks have drawn the attention of many pavement engineers in the last decades. Thermal cracking manifests itself in two ways: thermal fatigue cracking and low temperature cracking. The former is the result of cyclic thermal changes within the pavement and the latter can result from a single drop in air temperature, which is low enough to generate thermal stresses that exceed the tensile strength of asphalt concrete. In either case, the thermal coefficient of asphalt concrete can be used for estimating the total volume change of the surface course under thermal differentials and hence generated thermal stresses.

Since mid-seventies the thermal fatigue cracking of asphalt concrete has been under observation and the main reason for development of sever transverse cracks in west Texas was attributed to this type of distress (*2*). In order to observe the factors affecting this phenomenon, it is possible to apply thermal cycles on asphalt concrete specimens in the laboratory. However, due to the low thermal conductivity of asphalt, this process will take a long testing time and high experimental costs for the engineers (*3*). One way of considering thermal fatigue in pavement design is to use numerical models for estimating the time series of temperature and computing the thermally induced strains (*4*). It is believed that the thermal fatigue cracking in asphalt concrete is dominated by the high cyclic strain/stress levels induced in the flexible pavements rather than merely being controlled by the frequency of thermal cycles (*5*). Thermal fatigue occurs in the flexible pavements under very low loading frequencies; nonetheless, it is possible to mechanically simulate this phenomenon in the laboratory at relatively higher frequencies (*6*). It is worth noting that the simulated thermal frequencies in the laboratory are still much smaller than the frequencies related to the load-associated fatigue. As a result, only a few researches concerning the thermal fatigue were conducted in the laboratory through simulated mechanical application of thermal cycles at fairly low frequency levels; these studies were performed at constant strain modes and temperatures by using either two-point (*7*) or four-point bending beam fatigue tests (*6*). Since the thermal fatigue occurs in the temperature range of -7°C to 21°C (*2*), it would be wise to select a temperature that is within the suggested range. It should be kept in mind that the selection of a temperature close to the lower limit will result in a brittle fatigue behavior and selecting a temperature close to the upper limit makes the fatigue behavior to be dominated by relaxation.

It is known that aggregate type together with different gradations, asphalt type, asphalt content and modification affect the thermal cracking resistance of asphalt concrete. In terms of aggregate, it is believed that the gap-graded aggregates outperform the dense graded ones in the context of thermal fatigue performance (*7*). In addition, if the degree of interlock in aggregate structure increases, it will improve the thermal strength of asphalt concrete (*8*). As for the asphalt type, higher penetration grades result in sustaining more number of cycles before failure (*9*. Binders with lower stiffness cause the asphalt concrete to better resist against thermal cracking (*10*). If the asphalt content increases in the asphalt mixture, its resistance against thermal fatigue cracking improves proportionately (*6*). In terms of modification, it is believed that if modifiers are added to binder they can increase the thermal fatigue life of asphalt concrete (*7*). The wax crystallization in the bitumen microstructure was also found to be important to develop thermal fatigue in the binder domain of asphalt concrete (*11*).

In this study, in addition to testing the beam specimens consisting of different mixture variables, a thermal stress restrained specimen test (TSRST) setup was revised to determine the thermal fatigue resistance of asphalt concrete specimens, and then three response variables were identified to characterize the thermal fatigue resistance of each specimen. Finally, statistical analyses were conducted to determine the significant mixture design parameters for the thermal fatigue resistance of test specimens.

MATERIALS AND METHOD

Mixture design variables used in this study consisted of two types of aggregate: limestone, basalt; two gradations: coarse, fine (Figure 1), two types of asphalt grade: PG64-22, PG58-22; three asphalt contents: optimum and the optimum ±0.5%; and finally, some of the binders used were modified with SBS and the rest were left as virgin. The properties of aggregates and asphalt binders used can be observed from Table 1.

TABLE 1 Properties of aggregate and asphalt binder.

Aggregate	Specific gravity	Absorption (%)	LA Abrasion (%)
Limestone	2.75	1.45	28
Basalt	2.93	1.00	15

PG grade	Penetration value (0.1mm)	Specific gravity (g/cm^3)	Penetration grade
PG64-22	54	1.025	50/70
PG58-22	73	1.034	70/100

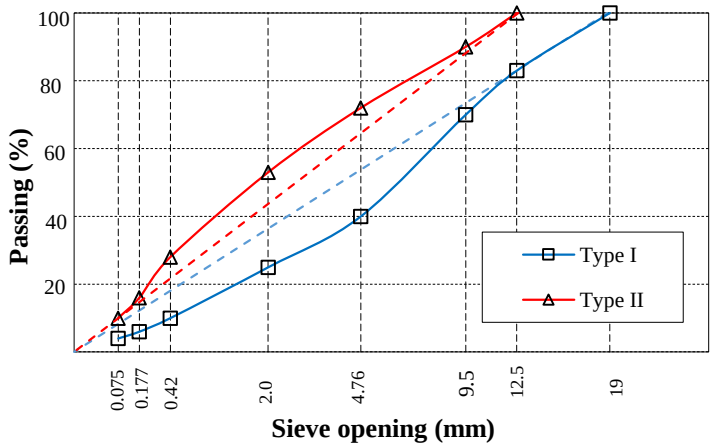


FIGURE 1 Aggregate gradations.

After preparation of the test mixtures they were age-hardened for three hours in the oven for the sake of achieving short term aging; then they were compacted using a French (LCPC) slab compactor. After the compaction process, the prismatic beam specimens with dimensions of 50×65×250 mm were cut out of the slabs using a diamond saw. After the cutting process, a portion of the specimens were used in a different testing program investigating the thermal fracture behavior of asphalt concrete. The remaining ones were, however, maintained in the laboratory at ambient temperature for 5 years to be tested for the thermal fatigue resistance. This long period let the specimens be naturally age-hardened rather than under accelerated oven aging. Previous studies indicate that the thermal fatigue cracking of asphalt concrete is not a viable mode of distress unless it is age-hardened (*3*). After the long-term aging process, the specimens were glued at both ends to steel platens using a high strength epoxy, and then installed into the TSRST device for the measurement of their thermal properties, i.e., thermal coefficient and subsequently thermal fatigue resistance.

In this study, along with the preparation of the test specimens, the most frequent daily temperature range during a 13-year period was determined for the city of Ankara, and a TSRST machine was calibrated in order to measure both the thermal coefficients, and the thermal fatigue resistance of each beam specimen. A sketch of the TSRST device can be seen in Figure 2 showing the components of the test frame. The thermal coefficients were measured to calculate the amplitude of cyclic thermal strains that were mechanically applied to each specimen for the purpose of evaluating its thermal fatigue performance at the selected frequency and the test temperature. It can be seen that the TSRST machine was fabricated from a steel frame and for ensuring insulation against heat loss, its internal walls were lined with a foam material of 6 cm thickness. The load cell measuring the force that is generated during thermal shrinkage was also insulated with the same foam material of at least 20 cm thickness from the cooling section of the chamber. A computer and a data acquisition system were connected to the TSRST machine in order to control the tests and record the data during the experiments. In order to control and record the surface temperature, 4 RTDs were attached on each surface of the beam specimens. A probe RTD was also fixed inside a dummy specimen for measuring the core temperature during testing.

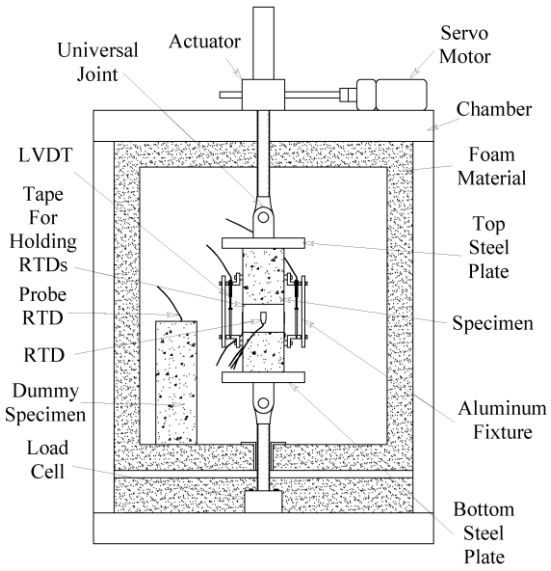


FIGURE 2 The schematic of the TSRST machine used for measuring the thermal coefficients and thermal fatigue performance of asphalt concrete specimens.

Selection of the Temperature Range to Calculate Strain Amplitudes

Because of the diurnal cyclic temperature changes, flexible pavements like the other types undergo thermal fatigue cracking during their service lives. For simulating this type of distress, it was necessary to find a temperature range in which this type of distress could be evaluated in the laboratory. As a result, for investigating the effect of thermal fatigue in flexible pavements, the weather data for the city of Ankara between 2000 - 2013 years were obtained from the Weather Bureau of Turkey. The data were then analyzed to find the frequency of temperature differentials only between -7 ºC and +21 ºC. For the thermal fatigue tests, the temperature differential (ΔT) with the highest frequency was selected to compute the strain amplitudes. Analysis of the weather data showed that for the city of Ankara, the most frequent temperature differential between -7 +21 ºC becomes ΔT = 10 ºC, as shown in Figure 3. It can be observed that the frequency of temperature ranges more than 10 ºC is also significant; however, because of the long test durations needed in thermal fatigue tests, only a single temperature differential had to be considered in the experiments.

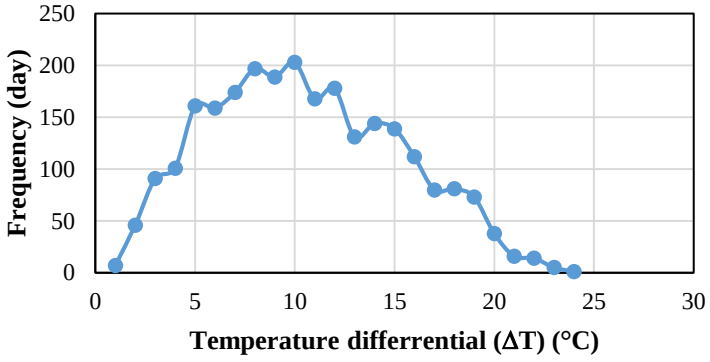


Figure 3 Analyzed weather data of the city of Ankara for the most frequent temperature cycle.

Measurement of Thermal Coefficients of Test Specimens

In order to measure the thermal coefficients, the beam specimens stuck between the steel platens were mounted in the TSRST machine and were conditioned at 15°C for three hours to achieve the thermal equilibrium. After the preconditioning period, the environment temperature was dropped at the rate of 10°C/h starting from 15°C and ending at -25°C. The selected rate of reduction of temperature was slow enough to ensure the uniform changes in

temperature within the specimens (*12*). During the tests, the axial deformation and the measured temperatures from each RTD were logged in every 30 seconds.

To determine the thermal fatigue resistance of the specimens under constant amplitude sinusoidal loading, at first the thermal coefficient of each specimen must be measured, so that the strain amplitudes could be calculated for a temperature differential of 10°C, as described in the above section. To achieve this, the strain and the temperature data were fit to a five-parameter model in Equation (1) using the least square method (*11,15&16*).

$$\varepsilon_l = \frac{\Delta l}{l_o} = C + \alpha_g (T - T_g) + R(\alpha_l - \alpha_g) \ln\left[1 + \exp\left(\frac{T - T_g}{R}\right)\right] \quad (1)$$

where: ε_l = linear strain at temperature T; C = intercept constant of the model; T_g = glass transition temperature; R = constant defining the curvature; α_l = thermal expansion coefficient for $T>T_g$; and α_g = thermal expansion coefficient for $T<T_g$.

During the measurement of the thermal coefficients, it has to be kept in mind that the thermal behavior of asphalt mixture can transform from rubbery into glassy state, as characterized by the existence of a glass transition temperature. For example, as it can be seen from Figure 4, there is a slight curvature at -12°C indicating the existence of a glass transition point in the applied temperature range. In this case, two thermal coefficients before and after the glass transition temperature are calculated, as indicated by the coefficient α_g and α_l in Equation (1), respectively. Because of the selected temperature range (10°C), and the test temperature (5°C) in the thermal fatigue testing, Equation 1 was used to calculate only the thermal coefficients falling above the glass transition temperature.

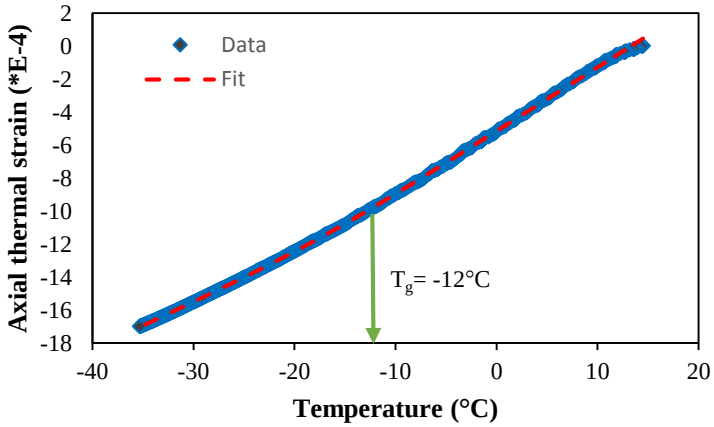


FIGURE 4 The data recorded for one of the specimens during the measurement of thermal coefficients.

After the measurement of the thermal coefficients, the thermal strains were calculated using Equation (2). Table 3 lists the calculated maximum thermal strains to be applied during testing for the beam specimens.

$$\varepsilon = \alpha_{\text{asphalt}} \Delta T \quad (2)$$

where: ε = thermal strain at the selected temperature range; α = thermal coefficient of contraction for beam specimens; and ΔT = temperature differential, for which the stain magnitudes are calculated.

Based on the calculated strains from Equation (2), the maximum and minimum strain levels defining the strain amplitude were chosen. In this study, it was assumed that the minimum strain level is zero implying a complete strain reversal, only at the initial cycle, for each load application. The maximum strain level was, however, chosen by the result of Equation (2) for the selected temperature differential of 10 °C. The applied sinusoidal (0.01Hz) strain waveform as defined by the max. strain ε_{max}, min. strain ε_{min}, and the loading frequency f can be seen from Figure 5.

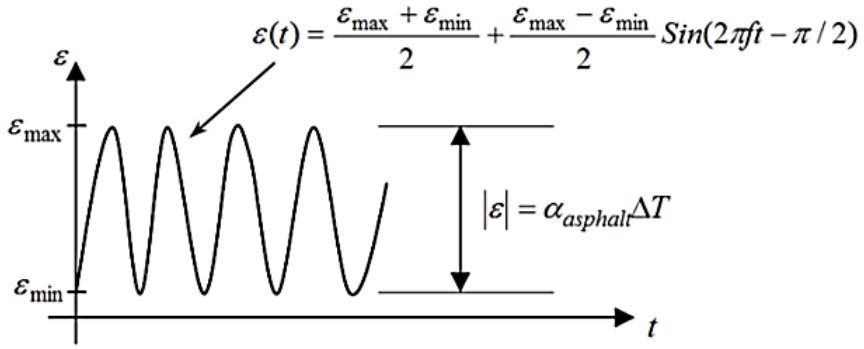


Figure 5 Waveform for the constant amplitude sinusoidal strain loading.

Table 2 Measured thermal strains

Specimen Code	Air void (%)	Thermal Strain (µm/m)	Specimen Code	Air void (%)	Thermal Strain (µm/m)
LF54ZO	2.8	333	LF73ZO-	3.6	407
LF54ZO	2.7	298	BF54ZO+	8.8	361
LF54ZO+	1.7	379	BF54ZO+	7.7	385
LF54ZO+	1.7	380	BC73ZO-	6.1	386
LC54SO-	4.4	347	BC73ZO-	5.7	384
LC54SO-	5.0	337	BC73ZO-	7.3	387
LF54SO+	4.4	374	BF73ZO+	6.8	388
LF54SO+	4.2	377	BF73ZO+	8.0	384
LF54SO+	2.5	367	BF73ZO-	10.2	305
LF73ZO	3.3	355	BF73ZO-	9.8	355
LF73ZO	2.9	382	BF73ZO-	10.9	376
LF73ZO	3.1	364	BC73SO+	2.2	444
LF73ZO-	4.7	385	BC73SO+	2.2	422

Note: B = basalt and L = limestone; C = coarse gradation and F = fine gradation; 54 = asphalt penetration value of 54(0.1mm) and 73 = asphalt penetration value of 73(0.1mm); S = asphalt modified with SBS and Z = no asphalt modification used; and O = optimum asphalt content, O- = asphalt content 0.5% less than the optimum and O+ = asphalt content 0.5% more than the optimum.

After the completion of the thermal fatigue tests, the stiffness reduction path for each specimen was calculated by dividing the peak-to-peak stress by the peak-to-peak strain to achieve the continuous monitoring of stiffness values as a function of loading cycles. In this phase, a separate algorithm was developed in the Matlab® environment to detect the correct peak to peak stress/strain of the same cycles. The thermal fatigue resistance of each specimen was then evaluated based on the selected three response parameters defined as 35 % reduction of its initial stiffness, 50% reduction of its initial stiffness, and the rate of reduction in the stiffness of the specimens. The dependence of these variables to air voids of the specimens was also investigated. The results of statistical analysis of variance on these response variables are presented in the next sections.

DATA ANALYSIS

Number of load cycles to 35% reduction of stiffness

In conventional load-associated fatigue tests, with the frequency range applied between 10-50 Hz, the criteria for ending the tests is either 50% reduction in stiffness or when the specimen breaks. However, in this study, due to the low frequency loads applied, it may not be feasible to carry on the tests until the reduction in the stiffness is reached to 50%. As a result, the tests were continued until either 72 hours for any specimen that did not break or approach to 50% of its initial stiffness. Up to 72 hours of load application, most of the specimens generally approached to stiffness reductions in the range of 35-50%. In the testing program, all of the test specimens could reach to 35 %

reduction in the stiffness, and hence the number load cycles at 35% stiffness levels are selected as one of the response parameters in the statistical analyses. Figure 6 presents the stiffness reduction path for three different specimens. As it can be seen in the figure, the paths represent the existence of uniform strain fields within the prismatic beam specimens (*9*).

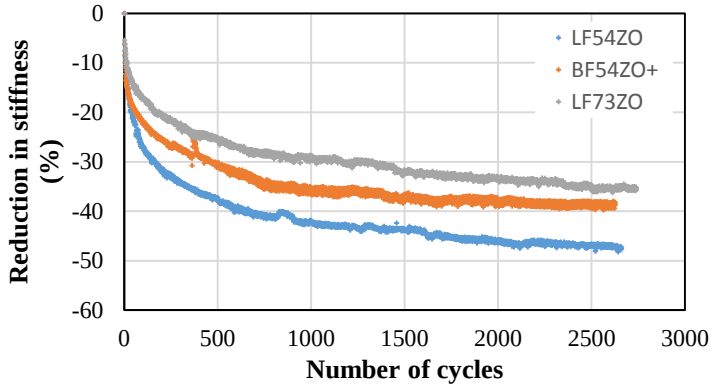


Figure 6 Stiffness reduction path for three different specimens.

Estimating number of cycles to 50% reduction of stiffness using a power model

Along with evaluating the fatigue life at 35% reduction in stiffness, it was decided to extrapolate the number of cycles to 50% reduction in stiffness using a power model conventionally used for modelling the traffic load-associated fatigue in Equation (3).

$$S = aN^{b} \tag{3}$$

where: S = stiffness at N^{th} cycle; and a, b = fatigue constants.

In order to fit the power model to the data, the stiffness reduction and the number of cycles were plotted in a log-log scale for each specimen, so that the model could be fitted to a portion of the gathered data representing the best fatigue behavior (Figure 7); as it is apparent in the figure, there are three regions; however, only the linear region was selected to represent the rate of stiffness reduction as an indication of fatigue resistance of the test specimens (*6*). The first portion is representative of an accelerating rate of reduction in stiffness which is due to the drastic changes in aggregate skeleton in the first few cycles; these changes are because of the big amplitude of the constant cyclic strains that were applied on the test specimens. The third part of the graph, in which the rate of stiffness reduction accelerates after a steady stage (2nd region), is attributed to the rapid crack growth within the specimen.

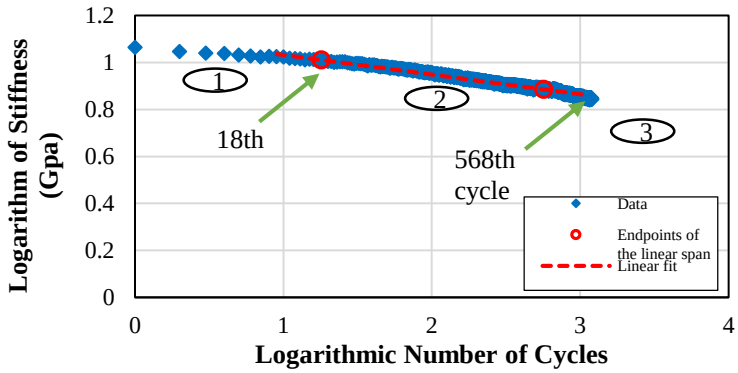


Figure 7 The data of stiffness versus number of cycles in a log-log scale.

The data plots in the log-log scale were observed visually to find a span representing the selected number of cycles belonging to the linear region. In order to exactly detect the location of the linear span, a code was written in the Matlab® environment to facilitate the fitting process. As it can be seen in Figure 7, the red line which is fitted to the data between the two circles represents the best linear fit for the selected fatigue data.

RESULTS AND DISCUSSION

The statistical analysis of variance tests (ANOVA) were conducted on the selected response parameters characterizing the thermal fatigue performance of the asphalt concrete specimens. ANOVA was performed for each parameter at 95% confidence level and the results are presented in Table 3. The significant mixture design variables for the thermal fatigue performance of the specimens can be identified by observing the probability (p) values whether or not it is lower than the selected confidence level of $(1-\alpha) = 0.05$. In the statistical analyses, the response parameters were selected from the number load applications up to the specified level of stiffness reductions. The first response parameter used is the number of load applications to 35% reduction in stiffness, as seen in Table 3. It can be noticed that the significant mixture design variable for this response parameter is the asphalt content with a probability level of 0.0055, even though the aggregate type and asphalt binder type seem also closer to the selected confidence level of 0.05. The graphical analysis for asphalt content can be observed from Figure 8 showing optimum minus 0.5% by O- through optimum plus 0.5% by O+. It can be seen that increasing the binder content increases the fatigue life of asphalt concrete; it is believed that the amount of air voids in the mixture affects the age hardening of the asphalt and if the asphalt content is increased, the binder becomes less prone to age hardening and hence the asphalt concrete sustains more number of thermal cycle before failure (*6*). The other reason could be the increased bonding between the aggregates when higher asphalt contents are used in the mixtures.

Table 3 Results of ANOVA analyses for the selected response parameters

Mixture Design Variable	35% Reduction in stiffness	50% Reduction in stiffness	Rate of stiffness reduction (*a*)
Aggregate type	0.0691	0.0539	0.0027
Gradation	0.6186	0.5288	0.333
Asphalt type	0.0621	0.5844	0.0845
Modification	0.3214	0.105	0.6419
Asphalt content	0.0055	0.0237	0.0611

The effect of mixture design variables on the thermal fatigue resistance for 50% reduction in stiffness can also be observed from second column of the Table 3. It is seen that as for the first response parameter, asphalt content again is the most significant parameter affecting the fatigue resistance of the specimens with a probability level of 0.0237. This significance level is slightly lower than for the first response parameter, however, the impact of asphalt content fatigue performance again remains for the test specimens. The graphical analysis of this response parameter in Figure 9 also shows a similar trend, as in Figure 8, except for one of the specimens (BF54ZO+).

The third response parameter (*a*) is the slope of the stiffness-number of load cycles relationship in the log-log scale, and indicates the rate of reduction in the stiffness of the specimens. The results of ANOVA for this parameter can be observed from Table 3. It can be noticed that the aggregate type is the most significant factor for the fatigue resistance of the test specimens with a probability level of 0.0027. The aggregates used in the testing program included limestone and basalt, normally displaying significant mixture performance under conventional load-associated fatigue tests performed under high frequencies. However, it appears that aggregate type becomes also a dominating mixture factor for the loading conditions under very low frequencies as applied in this testing program. The graphical analysis for this parameter is given in Figure 10. It is obvious that the rate of reduction in stiffness is higher for basalt aggregate than for limestone. This is expected due to the fact that limestone offers a better bonding with aggregate than for basalt, and therefore higher tensile strength to the mixture. Similar findings were also found in previous studies when the two aggregates were evaluated under low temperature cracking (*14*).

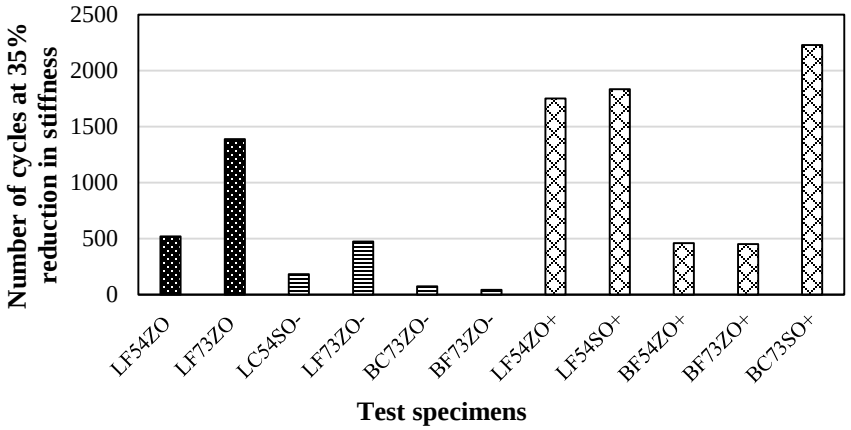


Figure 8 Average number of cycles to 35% reduction in stiffness calculated for asphalt content.

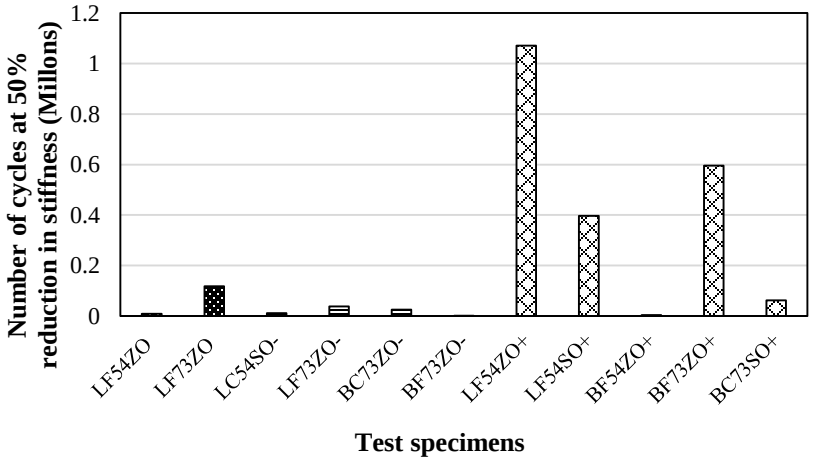


Figure 9 Average number of cycles to 50% reduction in stiffness calculated for asphalt content.

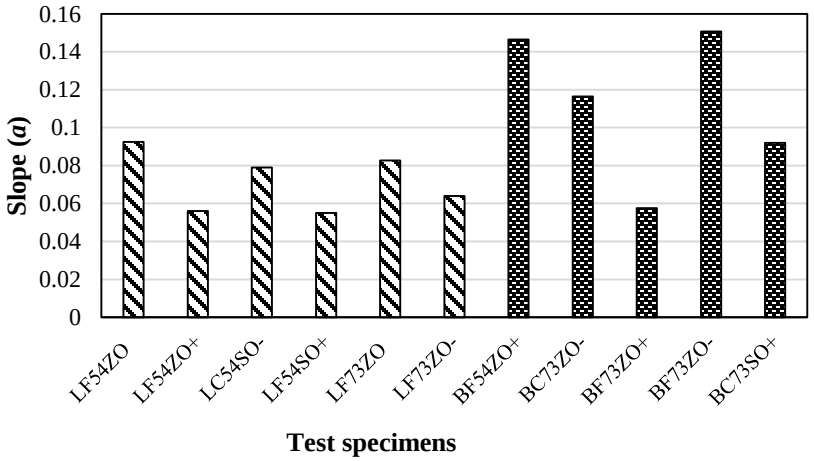


Figure 10 Average rate of reduction in stiffness calculated for aggregate type.

The impact of air void was also studied by plotting them for the number of loading cycles up to 35% stiffness reduction and the rate of stiffness reduction parameters. The plots can be observed from Figure 11 regardless of the mixture design combinations. It is clear that the measured fatigue performance of the specimens as characterized by their stiffness reductions up to 35% shows a strong correlation with air void contents. The trend reveals that higher air void will cause lower thermal fatigue performance as expected from the conventional fatigue tests results. Similarly, the rate of stiffness reduction seems to be accelerated by higher air void as can be observed from the same figure on the right. A careful observation of data from Table 2 indicates that the average air void for LC54SO-, BC73ZO-, and BF73ZO-, were measured 4.7%, 6.4%, 10.3%, respectively. The number loading cycles to 35% stiffness reduction was found low for these specimens (Figures 8 and 9) because of their weak microstructure as the result of high air void contents.

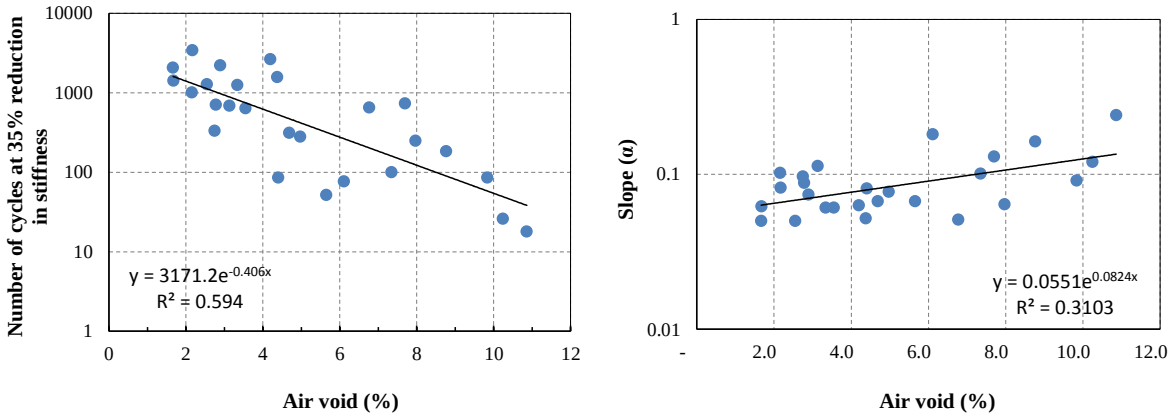


Figure 11 Effect of air void on thermal fatigue performance; i) up to 35% reduction in stiffness, ii) rate of stiffness reduction.

CONCLUSIONS

In this study, in order to the measure thermal fatigue resistance of asphalt concrete specimens a TSRST machine was revised to measure thermal fatigue performance of specimens under constant amplitude sinusoidal loading. The maximum strain levels used for each specimen were determined by the measured thermal coefficient using a temperature differential of 10 ^{o}C, as calculated for the city of Ankara. The result data obtained from the thermal fatigue tests were statistically analyzed for the selected response parameters to identify the effect of mixture design variables on the thermal fatigue performance of the test mixtures. The results of analyses led to the following outcomes:

- Asphalt content is the most significant mixture design factor for the thermal fatigue performance of the mixtures. Increasing asphalt content resulted in improved thermal fatigue resistance as indicated by the increased number load cycles to both 35% and 50% reduction in the stiffness of the specimens.
- Aggregate type proves to be a significant factor affecting the thermal fatigue resistance, in that limestone resulted in higher number of load cycles than for basalt for the same reduction level in mixture's stiffness.
- Even though the statistical analyses did not indicate aggregate type as significant factor for 35% and 50% stiffness reduction levels, it seems however, that the next important mixture design variable for thermal fatigue performance will be aggregate type given the probability levels calculated for this factor. Hence, further research is needed to investigate the effect of aggregate type on thermal fatigue performance of asphalt concrete.
- Air void content seems to have strong correlation with the number of loading cycles to the selected stiffness reduction levels and the rate of stiffness reduction regardless of the mixture type. Hence, as for the load inducted fatigue tests, air void content should also be taken into account in evaluating the thermal fatigue performance of asphalt concrete.

REFERENCES

1. Lytton, R. L., J. Uzan, E. G. Fernando, R. Roque, D. Hiltunen and S. M. Stoffels. *Development and Validation of Performance Prediction Models and Specifications for Asphalt Binders and Paving Mixes*. Strategic Highway Research Program, Washington, D.C., 1993.
2. Carpenter, S. H. Thermal Cracking in Asphalt Pavements: an examination of models and input parameters. USA CRREL, 1983.
3. Jackson, M. N., and T. S. Vinson. Analysis of Thermal Fatigue Distress of Asphalt Concrete Pavements. In *Transportation Research Record: Journal of the Transportation Research Board, No 1545*, Transportation Research Board of the National Academies, Washington, D.C., 1996 pp. 43-49.
4. Walther, A., and M. Wistuba: Mechanistic Pavement Design Considering Bottom-up and Top-down-Cracking. In Proceedings of seventh International RILEM conference on cracking in pavements, pp. 963-973, Netherlands, 2012.
5. Al-Qadi, I. L. , M. M. Hassan and M. A. Elseifi. Field and Theoritical Evaluation of Thermal Fatigue Cracking in Flexible Pavements. In *Transportation Research Record: Journal of the Transportation Research Board, No 1919*, Transportation Research Board of the National Academies, Washington, D.C., 2005 pp. 87-95.
6. Gerritsen, A. H., and D. J. Jongeneel. Fatigue Properties of Asphalt Mixes Under Conditions of Very Low Loading Frequencies. Shell international petrolum Company Limited, Amsterdam, The Netherlands, 1988.
7. Epps, A. L. An Approach to Examine Thermal Fatigue in Asphalt Concrete. *Journal of the Association of Asphalt Paving Technologists*, Vol. 68, 1999, pp. 319-348.
8. Tan, Y. Q., H. N. Xu, Z. J. Dong and W. Q. Gong: Effect of Aggregate Grading on Low Temperature Cracking Resistance In Asphalt Mixtures Based on Mathematical Statistics. Sixth International RILEM conference on cracking in pavements, Chicago, USA, 2008.
9. Lundstrom, R., H. D. Bendetto and U. Isacsson. Influence of Asphalt Mixture Stiffness on Fatigue Failure. *JOURNAL OF MATERIALS IN CIVIL ENGINEERING*, Vol. 16, 2004, pp. 516-525.
10. Roberts, F. , P. S. Kandhal, E. R. Brown, D. Y. Lee and T. W. Kennedy. *Hot Mix Asphalt Materials, Mixture Design, and Construction*. Second Edition NAPA Research andEducation Foundation ,Lanham, Maryland, 1996.
11. Das, P. K., D. Jelagin, B. Birgisson and N. Kringos: Micro-mechanical Investigation of Low Temperature Fatigue Cracking Behavior of Bitumen. In Proceedings of Seventh International RILEM conference on cracking in pavements, pp. 1281-1290, Netherlands, 2012.
12. Jung, D., and T. S. Vinson. Low Temperature Cracking Resistance of Asphalt concrete Mixtures. *Journal of the Association of Asphalt Paving Technologists*, vol. 62, 1993.
13. Bahia, H. U., and D. A. Anderson. Glass Transition and Physical Hardening of Asphalt Binders. *Journal of the Association of Asphalt Paving Technologies*, Vols. 62-93, 1993, pp. 93-129.
14. Guler, M., A. Qadir, , O. Demirel, A.G. Güngör , A. Hava, and M.V. Akpınar: Yol Kaplama Malzemelerinde Düşük Sıcaklık Çatlak Dayanımlarının Belirlenmesi, TÜBİTAK Project No: 105M193, 2010 Ankara, Turkey.
15. Tabatabaee, H. A., R. Velasquez, and H. U. Bahia. Modeling Thermal Stress in Asphalt Mixtures Undergoing Glass Transition and Physical Hardening. In *Transportation Research Record: Journal of the Transportation Research Board, No 2296*, Transportation Research Board of the National Academies, Washington, D.C., 2012 pp. 106-1014.
16. Bahia, H., H. Tabatabaee and R. Velasquez: Asphalt Thermal Cracking Analyzer (ATCA). Seventh International RILEM conference on cracking in pavements, pp. 147-156, Netherlands, 2012.